Anomalous Smoothing Preceding Island Formation During Growth on Patterned Substrates

R. Bergamaschini,[1] J. Tersoff,[2,*] Y. Tu,[2] J. J. Zhang,[3,4] G. Bauer,[3] and F. Montalenti[1]

[1]L-NESS and Dipartimento di Scienza dei Materiali, Università di Milano-Bicocca, Via Cozzi 53, 20125 Milano, Italy
[2]IBM T. J. Watson Research Center, Yorktown Heights, New York 10598, USA
[3]Institute of Semiconductor and Solid State Physics, University Linz, A-4040 Linz, Austria
[4]Institute for Integrative Nanosciences, IFW Dresden, Helmholtzstr. 20, D-01069 Dresden, Germany

(Received 17 July 2012; revised manuscript received 31 August 2012; published 9 October 2012)

We show that on suitably pit-patterned Si(001), deposition of just a few atomic layers of Ge can trigger a far larger flow of Si into the pits. This surprising effect results in anomalous smoothing of the substrate preceding island formation in the pits. We show that the effect naturally arises in continuum simulations of growth, and we identify its physical origin in the composition dependence of the surface diffusivity. Our interpretation suggests that anomalous smoothing is likely to also occur in other technologically relevant heteroepitaxial systems.

DOI: 10.1103/PhysRevLett.109.156101 PACS numbers: 68.55.−a, 81.15.Aa, 81.16.Nd

More than fifty years ago, Mullins showed that the corrugation amplitude of a nonplanar surface decays exponentially with time, driven by the reduction of surface energy and mediated by surface diffusion [1]. This is a fundamental effect in surface physics, quoted in textbooks, and because the smoothing becomes much faster with decreasing wavelength, it is particularly dramatic at the nanoscale. This effect has gained increasing technological importance with the use of patterned substrates to control the growth of semiconductor nanostructures [2–5]. Of particular interest for applications [2] is the possibility to exploit suitable patterns to enhance lateral ordering of Stranki-Krastanow islands [3,6]. Such applications generally involve heteroepitaxy, i.e., depositing a material different than the substrate. This introduces a host of new physical effects, including entropy of mixing, misfit strain, surface segregation, and mobility differences [2,5,7–11]. Despite an extraordinary amount of experimental and theoretical investigation, our understanding of the interplay between these factors is still incomplete.

Here we identify an anomalously rapid smoothing during the initial stages of heteroepitaxy on patterned substrates, and explain its origin. Understanding and controlling diffusion is important for any fabrication technology where the diffusion length during processing becomes comparable to the device structures. Diffusion takes on added importance in semiconductor heteroepitaxy because the shape evolution is closely coupled with alloy intermixing [9,12], and the electronic properties are very sensitive to both of these.

The deposition of Ge on patterned Si(001) substrates has been studied extensively (e.g., Refs. [3,6,13]). Hints that there may be an unexpected and unexplained smoothing can be found already in Ref. [14]. To investigate the behavior more systematically, two samples were grown by solid-source MBE on Si(001) substrates that had been patterned with a square array of roughly circular pits with a period of 500 nm using holographic lithography. Before growth, the pits had a depth and width about 65 and 350 nm, respectively. A 50 nm thick Si buffer layer was then deposited at a growth rate of 1.0 Å/s while ramping the substrate temperature T from 450 to 550 °C. After buffer growth, the substrate temperature was raised to $T = 720$ °C and stabilized (at the same T) for 30 s. For one sample, the substrate temperature was then immediately cooled to room temperature, and for the other sample it was cooled to room temperature after a deposition of 3.5 monoatomic layers (ML) of Ge at a rate $\Phi = 0.03$ Å/s at $T = 720$ °C.

The resulting profiles are shown in Fig. 1. Atomic force microscopy (AFM) images of pit arrays obtained after Si buffer-layer growth and after the subsequent Ge deposition are shown in Figs. 1(a) and 1(b), respectively, and enlarged single pits are shown in Figs. 1(c) and 1(d). Prior to Ge deposition, the Si buffer in Fig. 1(c) exhibits a multifaceted profile, with the the surface orientation map (SOM) in Fig. 1(e) clearly showing {001}, {11n}, {113}, and {15 3 23} facets [12,15]. After the subsequent deposition of 3.5 ML of Ge, the multifaceted pits transform into much shallower pits as seen in Fig. 1. Evidently, this small amount of Ge causes a major volumetric flow of material from the upper surface into the pit. Both the shape change and the net smoothing are evident in Fig. 1(g), which compares AFM linescans obtained after Si buffer-layer growth and after the subsequent deposition of 3.5 ML of Ge. Based on the small amount of Ge deposited (about 0.5 nm) relative to the smoothing, it is clear that the material accumulated in the pits must be highly diluted. By comparing AFM profiles before and after complete removal of the SiGe material by selective etching in a mixed solution of HF : H_2O_2 : CH_3COOH (1:2:3) [16,17], we estimate this material to be roughly 10% Ge.

To understand this surprising behavior, we carry out computer simulations of the growth process. Our model

 © 2012 American Physical Society

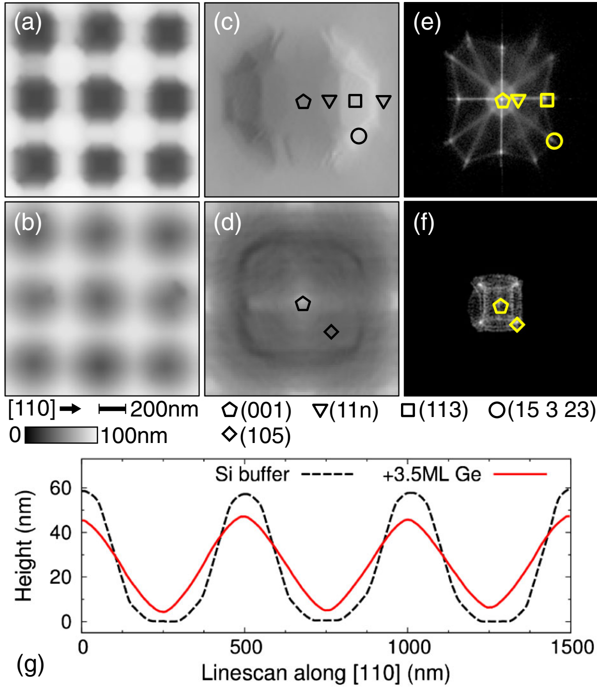

FIG. 1 (color online). AFM images of patterned substrates showing (a,b) pit array, and (b,c) enlarged view of single pit. Images (a) and (c) are obtained after the deposition of 50 nm of Si buffer, and (b,d) after the subsequent deposition of 3.5 ML of Ge at 720 °C. The corresponding distribution of surface orientations (e,f) shows which facets are present. (g) AFM linescans passing through pit centers along the [110] direction, for pits shown in (a) and (b). Vertical offset between curves is arbitrary.

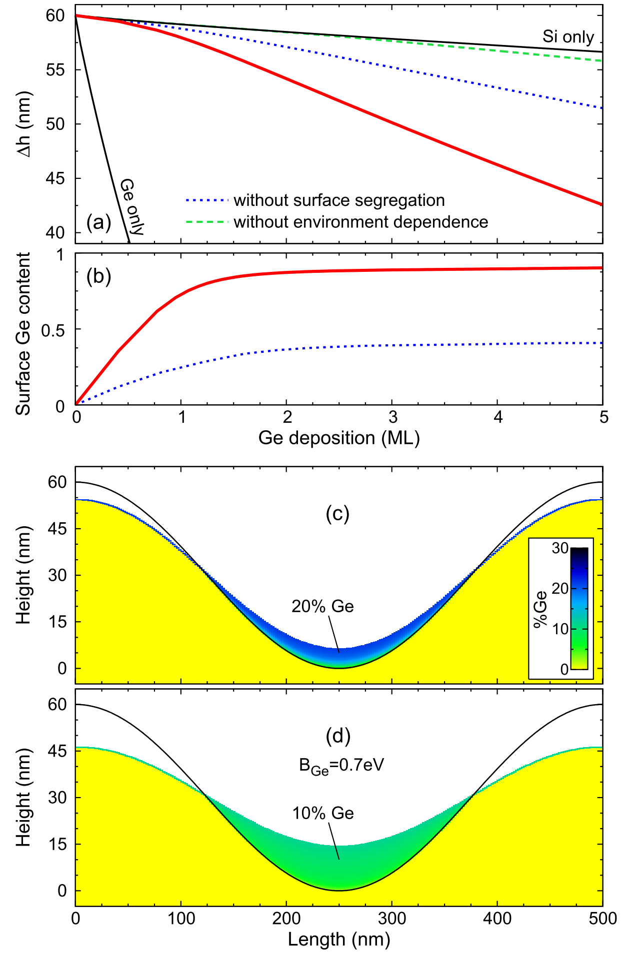

FIG. 2 (color online). (a) Decay of surface corrugation amplitude during Ge deposition. The solid red curve is the full calculation. The dashed curve shows the behavior if we omit the dependence of energy barriers on local composition; omitting Ge surface segregation but including the c dependence gives the dotted curve. Results for Si/Si and Ge/Ge are shown (labeled) for reference. (b) Evolution of composition of the topmost monoatomic layer during growth. Curves show the behavior including or omitting surface segregation as in (a). (The surface composition is uniform to within 1% across the surface; the average is shown.) (c) Pit profile and composition map after the deposition of 3.5 ML of Ge. (In showing the surface region we exclude the topmost atomic layer, which is roughly 85% Ge.) (d) Same result but assuming a lower value of the Ge diffusion barrier. For reference, the initial pit profile is included as a line in (c) and (d). Misfit strain has been neglected.

has been described previously [8,9,18,19], and further details are given in Ref. [20]. In brief, the system evolves by surface diffusion, while bulk diffusion is assumed to be negligible. Atoms within a few atomic layers of the surface are generally more mobile than in the bulk [21], so we assume that atoms within a depth w_s are in local equilibrium with the diffusing species. We report results for $w_s = 3$ ML, but values of 2–5 ML give very similar behavior [20]. The free energy of this surface region includes the dependence of surface energy on surface composition. Then surface segregation occurs automatically, with a region of thickness $w_s/3$ (representing the topmost atomic layer) having a different composition than the remaining thickness $2w_s/3$ [19]. The composition and morphology evolve as coupled equations [18], reflecting the combined effects of deposition and surface diffusion. Surface diffusion is driven by gradients in chemical potential arising from elastic strain relaxation, entropy of mixing, and surface curvature and composition [18,19]. For simplicity the calculations are two dimensional.

In order to address the specific issues raised by the experiments, we use a more detailed and realistic model for surface diffusivity than in the previously cited simulations of heteroepitaxy. We model the surface diffusion coefficient D_ν for each component ν (Si or Ge) as $D_\nu(c) = r\exp(-B_\nu(c)/kT)$ where k is the Boltzmann constant, B_ν is an activation energy which depends on the composition c of the topmost surface layer [20], and the prefactor r is taken to be the same for Si and Ge and independent of composition.

In general Ge forms substantially weaker bonds than Si. We therefore expect the activation energy for both species to decrease when the surface is more Ge rich. In analogy

with a simple bond-breaking model, we take $B_\nu(c) = c_\nu E_{\nu,\nu} + (1 - c_\nu)E_{\nu,\bar{\nu}}$, where $E_{\nu,\nu}$ is the activation energy for surface diffusion on pure Si or Ge, and the Si-Ge term $E_{\nu,\bar{\nu}}$ is taken as the average of these. The actual diffusion process is quite complex, perhaps involving ad-dimers. In the absence of quantitative experimental information, we take $E_{\mathrm{Si-Si}} = 1.4$ eV and $E_{\mathrm{Ge-Ge}} = 1.0$ eV (similar to values in the literature [22]).

Our simple model is intended only to qualitatively capture one essential aspect of the real, complex [23,24] behavior: the diffusivity of both species is expected to increase when the surface on which they move becomes enriched with the species that forms weaker bonds, in this case Ge. Such behavior may be rather general in semiconductor alloys, because weaker bonding at the surface tends to reduce the surface energy, driving surface segregation of that species.

For these calculations we choose an initial sinusoidal pattern mimicking the experimental one, and we deposit Ge at the experimental Φ and T. We first consider the simplest case, neglecting misfit strain and crystal anisotropy. Figure 2(a) shows the decay of the corrugation amplitude Δh, i.e., the height difference between the maximum and minimum along the profile. Figure 2(c) shows the resulting composition profile after the deposition of 3.5 ML of Ge. Although the diffusing material is 80% Si, the smoothing is nearly an order of magnitude faster than for pure Si [as evident from the panel of Fig. 2(a)]. Thus the simulation clearly captures the striking phenomenon seen in the experiment.

To understand how a small Ge flux leads to such a large transfer of Si, we compare with calculations omitting key elements of the physics. A simpler approximation used in the literature is to take different species as having different mobilities (in the present case Ge atoms diffusing much faster than Si ones), but neglecting any dependence on the composition of the environment. The result is shown as a dashed curve in Fig. 2(a). In that approximation, Ge deposition has almost no effect on the rate of smoothing. Instead, the smoothing is controlled primarily by the slower-diffusing species, as discussed in Ref. [18]. If we include the composition dependence but omit surface segregation, then there is a substantial smoothing (dotted line), but still much less than in the full calculation. This is because the surface Ge composition is not as high without surface segregation, as shown in Fig. 2(b). Thus, the anomalous smoothing observed in the experiments is mostly determined by the dependence of the Si diffusivity on the surface composition, but the effect has a strong synergy with surface segregation.

The role of surface composition and surface segregation can be seen in more detail by comparing Figs. 2(a) and 2(b). At the beginning the surface is nearly pure Si. This gives a slow evolution, comparable to annealing pure Si. Over the first ~1 ML of Ge deposition, the surface composition rises rapidly in Fig. 2(b), and there is a corresponding increase in the slope (rate of smoothing) in Fig. 2(a). At less than 2 ML of Ge, the system has already reached a quasi-steady state where the surface Ge content is increasing only very slowly, and the profile decay rate is relatively constant.

Given the simplicity of our model and the complexity of real Ge/Si(001) surfaces, we cannot expect quantitative agreement with the experiment, and we have focused on qualitative aspects of the behavior. Nevertheless, it is interesting to note that we can obtain better agreement with the experimental results of Fig. 1 by further lowering the Ge activation energy. In Fig. 2(d) we show results for B_{Ge} reduced to 0.7 eV. All other parameters are as in Fig. 2(c). The same 3.5 ML of Ge deposition leads to a much greater smoothing than in Fig. 2(c). In this case the material filling the pit is only around 10% Ge, similar to what is seen in the experiment. It is difficult to assess what parameter values are most reasonable in the absence of a detailed microscopic understanding of diffusion of both species at arbitrary surface compositions. Still, the results displayed in Fig. 2(d) highlight the possible extent of the anomalous pit-filling effect, especially for systems with large differences in surface bond strength.

In the absence of other effects, the anomalous smoothing would continue toward the complete flattening of the profile, as shown in Fig. 3(a). However, in most heteroepitaxial systems there is some misfit strain, e.g., a 4% difference in lattice constant between Ge and Si. This strain eventually leads to island formation, whether on flat or patterned surfaces, unless relieved by misfit dislocations [2]. In Fig. 3, we continue the simulation of Fig. 2 to higher Ge coverage. If we omit any misfit, the smoothing continues at a steady rate, Figs. 2(a) and 3(a). The realistic case including misfit strain and elastic relaxation is shown in Fig. 3(b). Comparing the two, we see that there is no noticeable difference in the earliest stages, e.g., at 2 ML of Ge. This is an example of the more general scaling law: the strain energy is relatively unimportant for volumes small compared to a strain-dependent size scale [25]. Thus strain is not a significant factor in the initial anomalous smoothing.

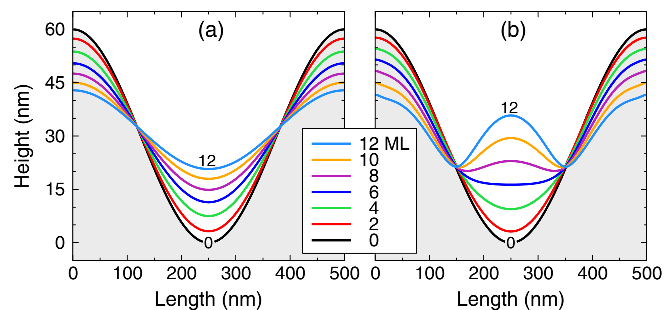

FIG. 3 (color online). Evolution of the pit profile for later stages of Ge deposition comparing the cases (a) without misfit strain and (b) including misfit. The grayed area represents the initial cosine pit profile.

However, with further deposition, strain becomes increasingly important relative to surface energy. We see in Fig. 3(b) that the pit bottom tends to flatten and finally an island appears at the center of the pit [26], growing toward higher aspect ratio with increasing volume [15,25].

A striking feature in the experiments of Fig. 1 is the facet structure before and after Ge deposition. To test whether our conclusions are sensitive to faceting, we repeat the calculations for an anisotropic surface energy, $\gamma(\theta) = \bar{\gamma}[1 - \alpha \cos(32\theta)]$ with $\alpha = 10^{-3}$. This gives "facets" at around 11° and 22°, in analogy with the {105} and {113} facets in the experiment, and adequately describes some key experimental features of this system [27].

Starting from the same sinusoidal Si profile as before, we anneal at 720 °C for 5 s to obtain a faceted pattern on Si. If we then grow a Si buffer layer, Fig. 4(a), there is very little smoothing of the pattern—much less than for the isotropic model. The evolution under Ge deposition is shown in Figs. 4(b) and 4(c). Dramatic smoothing when Ge is deposited is again predicted. As in the experiment (Fig. 1), the smoothing leads to a pyramidal pit morphology consisting only of (001) and {105}-like facets, Fig. 4(c). Further deposition leads to a pyramidal island inside the pit, Fig. 4(d), again in agreement with the phenomenology observed in the experiment [2,15]. In Fig. 4(d) the island composition remains close to 20% Ge, as in the initial anomalous smoothing, while the experiments find islands more rich in Ge [12], but at this stage we do not know which aspects of the model account for this discrepancy.

We have focused on a single temperature, $T = 720$ °C. If we reduce the temperature, there are two effects: an increase in the ratio between Ge and Si diffusivities, but also a much larger absolute decrease in both. For example, if we lower T to 550 °C, the slower diffusion allows for little lateral transport during deposition, leading to a thin conformal Ge-rich layer in agreement with low-T experiments [14]. However, simulations performed lowering the deposition flux by a factor ~ 22 (corresponding to the lowering in average diffusivity) show a smoothing effect even larger than at 720 °C, as the difference in activation energies is larger relative to kT. Thus, by simultaneously varying T and Φ, one can control the extent of the anomalous smoothing.

The anomalous smoothing also depends on the initial geometry. For instance, preliminary experimental results (not shown) reveal strong anomalous smoothing for a pattern with pitch 270 nm and pit depth 50 nm, grown at $\Phi = 0.05$ Å/s, and $T = 640$ °C. Simulations reproduced again the observed behavior.

In conclusion, we have demonstrated the existence of an unexpected anomalous smoothing during the initial stages of Ge deposition on a patterned Si(001) substrate. We showed that such behavior arises naturally in our growth simulations, as a consequence of the reduced activation energy for diffusion of both Si and Ge when the surface is

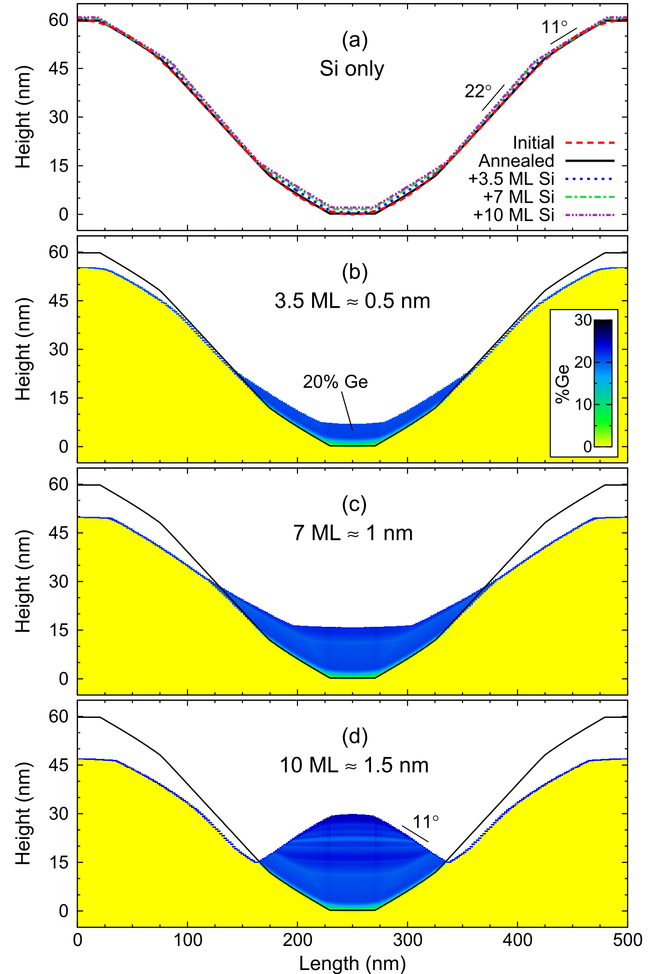

FIG. 4 (color online). Profile evolution including crystal anisotropy, starting with the same sinusoidal pit as before. (a) Evolution for pure Si. Annealing at 720 °C for 5 s gives a faceted profile. Other curves show the profile after the deposition of varying amounts of Si, as indicated, for comparison with Ge deposition. (b–d) Profile and composition maps at different stages of Ge deposition. For reference, the line shows the initial pit profile after annealing. (The topmost layer, ~85% rich in Ge, is not shown).

Ge enriched. This enrichment occurs quite early in the deposition due to surface segregation. As more Ge is deposited there is a crossover, from simple smoothing driven by surface energy, to strain-driven island formation in the centers of the pits. We anticipate that similar anomalous smoothing should occur for other systems, since a material that segregates to the surface due to weaker bonding will also generally be favorable for fast diffusion of both species. More quantitative modeling will require advances (along the lines of Refs. [28]) in the understanding of basic materials properties, such as the dependence of surface-energy anisotropy on surface composition and strain.

We gratefully acknowledge scientific discussions with A. Rastelli, M. Brehm, M. Grydlik, and Leo Miglio.

*tersoff@us.ibm.com

[1] W. W. Mullins, J. Appl. Phys. **28**, 333 (1957).
[2] J. Stangl, V. Holý, and G. Bauer, Rev. Mod. Phys. **76**, 725 (2004).
[3] Z. Zhong and G. Bauer, Appl. Phys. Lett. **84**, 1922 (2004).
[4] E. Kapon, M. Walther, J. Christen, M. Grundmann, C. Caneau, D. M. Hwang, E. Colas, R. Bhat, G. H. Song, and D. Bimberg, Superlattices Microstruct. **12**, 491 (1992).
[5] G. Biasiol and E. Kapon, Phys. Rev. Lett. **81**, 2962 (1998); E. Pelucchi, V. Dimastrodonato, A. Rudra, K. Leifer, E. Kapon, L. Bethke, P. A. Zestanakis, and D. D. Vvedensky, Phys. Rev. B **83**, 205409 (2011).
[6] S. Kiravittaya, A. Rastelli, and O. G. Schmidt, Appl. Phys. Lett. **87**, 243112 (2005).
[7] G. Medeiros-Ribeiro and R. S. Williams, Nano Lett. **7**, 223 (2007).
[8] B. J. Spencer, P. W. Voorhees, and J. Tersoff, Phys. Rev. B **64**, 235318 (2001).
[9] Y. Tu and J. Tersoff, Phys. Rev. Lett. **98**, 096103 (2007).
[10] P. Venezuela and J. Tersoff, Phys. Rev. B **58**, 10871 (1998).
[11] G. Chen, B. Sanduijav, D. Matei, G. Springholz, D. Scopece, M. J. Beck, F. Montalenti, and L. Miglio, Phys. Rev. Lett. **108**, 055503 (2012).
[12] J. J. Zhang, F. Montalenti, A. Rastelli, N. Hrauda, D. Scopece, H. Groiss, J. Stangl, F. Pezzoli, F. Schäffler, O. G. Schmidt, L. Miglio, and G. Bauer, Phys. Rev. Lett. **105**, 166102 (2010).
[13] G. Chen, H. Lichtenberger, G. Bauer, W. Jantsch, and F. Schäffler, Phys. Rev. B **74**, 035302 (2006).
[14] M. Grydlik, M. Brehm, F. Hackl, H. Groiss, T. Fromherz, F. Schäffler, and G. Bauer, New J. Phys. **12**, 063002 (2010).
[15] J. J. Zhang, M. Stoffel, A. Rastelli, O. G. Schmidt, V. Jovanović, L. K. Nanver, and G. Bauer, Appl. Phys. Lett. **91**, 173115 (2007).
[16] U. Denker, A. Rastelli, M. Stoffel, J. Tersoff, G. Katsaros, G. Costantini, K. Kern, N. Y. Jin-Phillip, D. E. Jesson, and O. G. Schmidt, Phys. Rev. Lett. **94**, 216103 (2005).
[17] T. K. Carns, M. O. Tanner, and K. L. Wang, J. Electrochem. Soc. **142**, 1260 (1995).
[18] J. Tersoff, Appl. Phys. Lett. **83**, 353 (2003).
[19] Y. Tu and J. Tersoff, Phys. Rev. Lett. **93**, 216101 (2004).
[20] See Supplemental Material at http://link.aps.org/supplemental/10.1103/PhysRevLett.109.156101 for further details of the model used here.
[21] B. P. Uberuaga, M. Leskovar, A. P. Smith, H. Jónsson, and M. Olmstead, Phys. Rev. Lett. **84**, 2441 (2000).
[22] D. J. Godbey, J. V. Lill, J. Deppe, and K. D. Hobart, Appl. Phys. Lett. **65**, 711 (1994).
[23] R. W. Balluffi, S. M. Allen, and W. Craig Carter, *Kinetics of Materials* (Wiley, New York, 2005).
[24] L. Huang, F. Liu, G. H. Lu, and X. G. Gong, Phys. Rev. Lett. **96**, 016103 (2006). (Note that this work addresses adatom mobility, which is only one component of the total diffusivity.)
[25] B. J. Spencer and J. Tersoff, Phys. Rev. Lett. **79**, 4858 (1997); I. Daruka, J. Tersoff, and A.-L. Barabasi, Phys. Rev. Lett. **82**, 2753 (1999).
[26] L. Miglio and F. Montalenti, in *Silicon-Germanium (SiGe) Nanostructures: Production, Properties, and Applications in Electronics*, edited by Y. Shiraki and N. Usami (Woodhead Publishing, UK, 2011).
[27] J. Tersoff, B. J. Spencer, A. Rastelli, and H. von Känel, Phys. Rev. Lett. **89**, 196104 (2002).
[28] G. H. Lu and F. Liu, Phys. Rev. Lett. **94**, 176103 (2005); C. J. Moore, C. M. Retford, M. J. Beck, M. Asta, M. J. Miksis, and P. W. Voorhees, Phys. Rev. Lett. **96**, 126101 (2006).